The ecological dynamics and consequences of phytoplasma in a spring ephemeral

Julia A. Boyle[1,2], Yanggaolan Yang[3], Amalia Caballero[4], Eleanor N. Hector[2,5], Alex Ellett, Emily Glasgow[2], John R. Stinchcombe[2,6], Megan Bontrager[2]

[1] Department of Ecology and Evolutionary Biology, University of Michigan, 1105 N University Ave, Ann Arbor, MI, 48109, USA

[2] Department of Ecology and Evolutionary Biology, University of Toronto, 25 Willcocks St., Toronto, ON, M5S3B2, Canada

[3] Department of Biology, Queen's University, 99 University Ave, Kingston, ON, K7L 3N6, Canada

[4] Department of Molecular Genetics, University of Toronto, Medical Science Building, 1 King's College Cir Room 4386, Toronto, ON M5S 3K3, Canada

[5] Department of Zoology, Biodiversity Research Centre, University of British Columbia, Vancouver, BC V6T 1Z4

[6] Koffler Scientific Reserve, University of Toronto, Toronto, ON Canada, M5S3B2

Abstract

Ecologists have long sought to link within-population dynamics to patterns of species occurrence and persistence across the range. Theoretical models suggest pathogens have important implications for plant populations and perhaps even limit plant distributions, though more empirical evidence is needed, especially in wild plant populations. In the field, we characterized the infection dynamics of phytoplasma, a vectored and sterilizing bacterial pathogen, in wild populations of white trillium. We identified the bacterial strain and local vectors. We then leveraged community science data to reveal patterns and potential drivers of phytoplasma occurrence across the range of white trillium. Within populations, we found that phytoplasma infection presence was more likely in low host density plots, where insect vectors occupied a higher proportion of trillium, indicative of an encounter-dilution effect. Leafhoppers in the genus *Empoasca* are the likely vectors of *Candidatus* Phytoplasma pruni-related, group 16SrIII infections between trilliums. Phytoplasma was widely distributed across trillium's range, even at range edges, and probability of infection was significantly reduced by hotter summer temperatures and increased by proximity to cropland. Our results suggest vectored pathogens are sensitive to local host population densities and able to persist across both the core and edge of host ranges.

Introduction

Understanding how within-population dynamics scale up to affect species' metapopulation dynamics and geographic distributions has been a central goal of ecological research for decades (Harrison and Taylor 1997, Freckleton et al. 2005, Oldfather and Ackerly 2019) and understanding the impacts of pathogens on these large-scale processes remains challenging (Gilbert 2002). Plant populations display density-dependent dynamics in interactions with competitors, pollinators, seed predators, herbivores, and others (Gilbert 2002, Gunton and Kunin 2009, Kim et al. 2013, Hegland 2014). The addition of phytopathogens may reinforce or disrupt a plant population's density-dependent processes (Parker and Gilbert 2018), which could lead to altered distribution patterns or demographic structure. Much of our understanding of plant pathogens comes from agricultural systems, but natural populations may have fundamentally different infection dynamics due to environmental and demographic heterogeneity (Alexander 2010). Disease dynamics in natural populations are also important because populations can act as reservoirs of pathogens (Webster et al. 2007, Petersen et al. 2019) and because disease outbreaks are a conservation concern, even for abundant plant species (Frankel 2008, Pautasso et al. 2013). Here, we characterise a pathogen in a naturally-occurring plant population and leverage community science data to evaluate whether population-level disease dynamics scale up across the range of the host species.

Pathogen success hinges on the properties of host populations, and host population density often plays an important role at a local scale (Burdon and Chilvers 1982). Density-dependent dynamics occur when transmission has a linear relationship with the absolute number of infected individuals (Antonovics 2017); positive density-dependence has been observed in many wild plant populations, often when pathogens are transmitted aerially or via direct contact

(Carlsson and Elmqvist 1992, Gilbert et al. 1994, Lively et al. 1995, Bell et al. 2006). Density-dependent transmission may result in different proportions of individuals infected at different host densities. In contrast, frequency-dependent dynamics occur when transmission increases with the proportion of hosts that are infected, instead of correlating with host density (Antonovics 2017, Antonovics et al. 2023). Over time, this may result in similar proportions of individuals infected across populations of differing density. While vector-transmitted pathogens are often considered frequency-dependent, they may possess qualities of both density-dependent and frequency-dependent transmission because transmission can initially increase as host density increases, but decrease at higher host density (Antonovics et al. 1995, 2017, 2023). Transmission may decrease at high host density because vectors are limited by time, satiation, or abundance, reducing the chance that a host interacts with a vector; this phenomenon is known as the encounter-dilution effect (Mooring and Hart 1992, Krebs et al. 2014). Recently, Antonovics and colleagues (2023) found that pollinators were more effective transmission vectors of anther-smut fungus at lower host densities compared to higher host densities, providing evidence of the encounter-dilution effect in plant-vector-pathogen interactions at relatively small spatial scales.

Scaling up phytopathogen dynamics from a local host population to explore patterns across a whole host range is empirically challenging and therefore, rarely done (Bruns et al. 2019a, Uricchio et al. 2023). Species ranges are often constrained by the climatic and resource parameters a species can tolerate (Lee-Yaw et al. 2016), and it remains an open question whether species interactions frequently expand or limit ranges and abiotic niches (Afkhami et al. 2014, Harrison et al. 2018, Uricchio et al. 2023, Nathan et al. 2023). Classic models with host-specific pathogens predict that regions of low host density, such as some range edges, should also have low pathogen loads due to positive density-dependence, forming a ‘disease-free halo’

(Antonovics 2009, Bruns et al. 2019a). However, frequency-dependent pathogens may be found even in areas of low host density. Bruns et al. (2019a) found that a vectored phytopathogen was maintained at a host's range limits and occurred at higher prevalence at range edges compared to range centres. Further work indicates that this pathogen constrains the range of a host species and may eventually lead to host range contraction or extinction (Uricchio et al. 2023). The persistence of plant populations at range edges is important for the ability of a species to shift ranges and respond to climate change (Rehm et al. 2015, Hargreaves and Eckert 2019), thus necessitating a deeper understanding of how pathogens affect plant populations across host ranges.

Almost 150 years ago, Erwin Smith described a "monstrous form" of *Trillium grandiflorum* (Smith 1879). Instead of the characteristic white blooms, Smith observed trillium with virescent petals and more numerous leaves held on longer petioles. While Smith suggested these plants might be taxonomically distinct entities, we now know that these morphological variations reflect symptoms of phytoplasma infection (Hooper et al. 1971). Phytoplasmas are bacterial parasites that live obligately in the intracellular phloem tissue of plants and the bodies of their insect vectors, which are often phloem-feeding insects in the order Hemiptera (Sinha and Chiykowski 1980, Lee et al. 2000, Wang et al. 2024). Vectors are exposed to phytoplasmas when they consume the phloem of infected plants (Christensen et al. 2005). Phytoplasmas have been found in over 1000 plant species including those used as timber, ornamental plants, and crops (Lee et al. 2000), yet their biology remains poorly understood (Liu et al. 2017). In addition to inducing morphological changes, phytoplasmas can sterilize their plant hosts and infection can be systemic and lifelong (Lee et al. 2000, Wright et al. 2022; Ustun et al. 2023). The longevity of infected perennial plants is consequential, as it means these individuals may act as a source of

infection for many years. *Trillium grandiflorum* is one such long-lived species; individuals become reproductive after 7-10 years, with a total lifespan of over 30 years (Hanzawa and Kalisz 1993, Lamoureux and Larose 2002). Theoretical models predict that sterilizing pathogens in small and long-lived host populations can drive host populations to extinction more often than lethal pathogens (Anderson & May 1981; Boots & Sasaki 2001; Gerber et al. 2005; Antonovics 2009). Thus, phytoplasma may have grave consequences for the persistence of trillium and other susceptible plants' populations. Smith's (1879) report of a trillium-dwelling phytoplasma was in Michigan, USA, suggesting this species interaction has long been established in northeastern America. Although the first Canadian confirmation of phytoplasma infection in trillium occurred in the last decade (Arocha-Rosete et al. 2016), observations of the symptoms of phytoplasma infection in Ontario were documented long before (Gates 1917). The phenotypic, fitness, and population-level effects of phytoplasma on trillium have never been quantified, thus characterizing these effects is one step towards determining if this pathogen poses a threat to trillium persistence or if they are stably co-existing.

We explored the links between phytoplasma infection and the performance, stage structure, and density of wild populations of the spring ephemeral *Trillium grandiflorum*. We further characterized the strain of phytoplasma and its insect vectors at our field site. We then leveraged community science data to examine how patterns in phytoplasma infection within plant populations scale up across the range of *T. grandiflorum*. We hypothesized that phytoplasma would reduce trillium fitness and reduce the relative abundance of earlier demographic stage classes within populations. Given that phytoplasma is vector transmitted, we hypothesized that its transmission would be primarily frequency-dependent, resulting in an equal chance and rate of infection in populations regardless of host density. However, we had an

alternative hypothesis that the encounter-dilution effect could reduce transmission at high host densities due to vector behaviour or limitation, resulting in a lower proportion of infected hosts, and more consistent with negative density-dependence. Finally, we predicted that phytoplasma infection would be prevalent even at range edges due to frequency dependent, vector-mediated transmission. Our work characterizes infection dynamics of a fearsome and understudied plant pathogen in a wild host population and across the host's range.

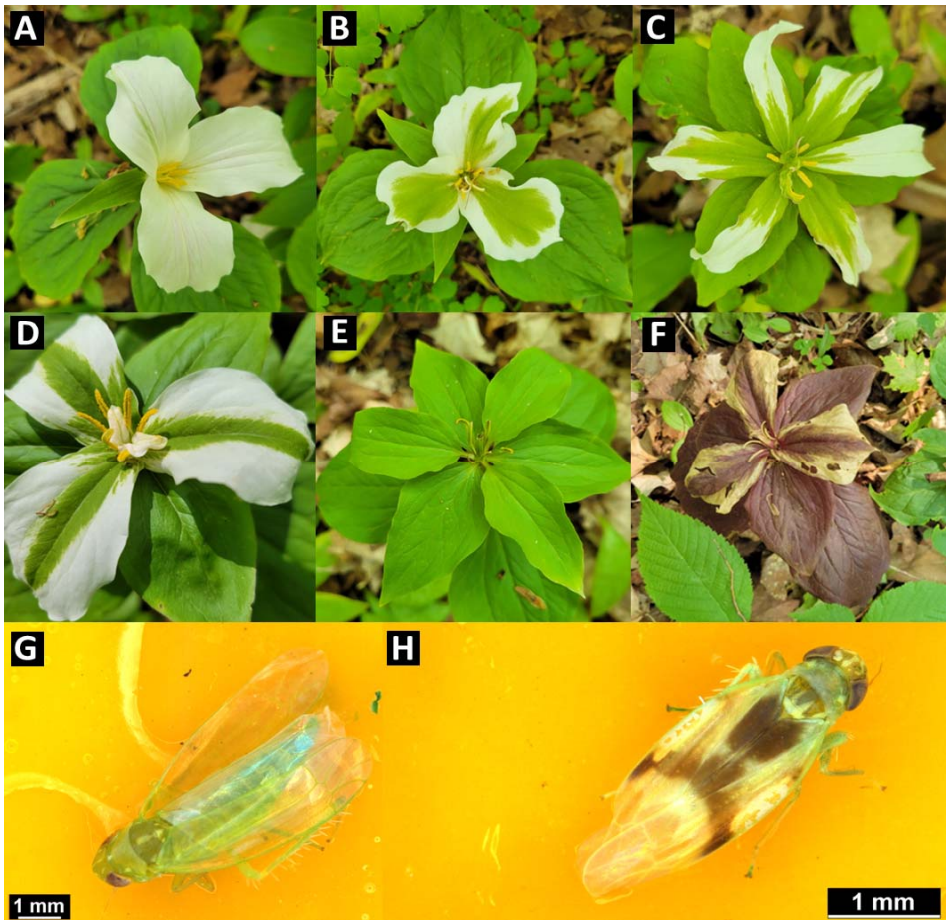

Figure 1. Diversity of phytoplasma infection symptoms in *Trillium grandiflorum* and two identified vectors. Symptoms include phyllody, virescence of petals, and larger sepals (A-E), as well as other deformations including extra petals (C) and the absence of pollen (E-F). Discolouration in an infected plant late in the flowering season (F). Using sticky traps, we

identified *Empoasca* spp. leafhoppers positive for phytoplasma (G, H). All photos by authors, images of *T. grandiflorum* were taken at the Koffler Scientific Reserve.

Methods

Study organisms and site

Trillium grandiflorum (white trillium) is a spring ephemeral native to the deciduous woodlands of eastern North America. Its range spans from Minnesota to the Eastern coast, and from Georgia to northern Ontario (Case 1993). *Trillium grandiflorum* reproduces by seed and clonal reproduction by rhizomes is rare (Ohara 1989); seeds of this species are frequently dispersed by ants over short distances (Kalisz et al. 1999). Trillium have four distinct demographic stages: a seedling stage, a single leaf vegetative stage, a three-leaf vegetative stage, and a reproductive stage (Ohara 1989, Rooney and Gross 2003). Once a trillium has first bloomed it often continues to bloom annually but can go dormant for one or more years (persisting as a rhizome with no aboveground structures) or revert to a three-leaf non-reproductive stage. In Ontario, white trillium begins flowering in mid-May and sets seed by July, after which the aboveground parts of the plant die back. There are large populations of wild *T. grandiflorum* at our study site (Figure S1), the Koffler Scientific Reserve (KSR, www.ksr.utoronto.ca) in Ontario, Canada (44°01'48”N, 79°32'01”W). Symptoms of phytoplasma infection have been observed in trillium populations at KSR since at least the early 2000s (A. Weis, personal communication). Phytoplasma infection is most apparent when the white trilliums are flowering, as petals will range from having a streak of green to full virescence or phyllody (Figure 1). The strain of phytoplasma previously identified in a different *T. grandiflorum* population was *Candidatus* Phytoplasma pruni-related, group 16SrIII, otherwise known as Western X-disease or peach X-disease (Arocha-Rosete et al. 2016).

Effects of phytoplasma infection on Trillium grandiflorum growth and reproduction

To investigate whether infection was associated with differences in plant size, we quantified total plant height, leaf length, and sepal length in symptomatic (n = 32) and asymptomatic (n = 30) trillium during peak flowering season (May 20-29, 2023) across 30 locations in an approximately 15-hectare section of mixed deciduous forest at KSR. We determined infection status by visually inspecting petals for virescence; we suspect that some infected individuals have no visible symptoms, so this method likely underestimates the overall infection rate of the population. To test for differences in plant size phenotypes associated with infection, we used linear mixed effects models with infection status as a predictor and location as a random effect. We applied a natural log transformation on responses as needed to improve normality. For statistical analysis, we used R v4.2.0 (R Core Team 2022), with the *tidyverse* (Wickham et al. 2019), *lme4* (Bates et al. 2015), and *lmerTest* (Kuznetsova et al. 2017) packages. All linear models were corrected using a type III ANOVA with the *car* package (Fox and Weisberg Sanford 2019).

To quantify differences in seed production due to infection, we first characterized the relationship between size and seed number in asymptomatic trilliums. We haphazardly sampled 100 individuals on 13 June 2024, aiming to maximize variation in plant size. On these plants we measured leaf length and seed set, then estimated the relationship between them using a generalized linear model with a Poisson family. Then, we counted the number of seeds produced by 81 haphazardly chosen symptomatic trillium in early to mid-June 2024. To estimate potential reproductive loss due to infection in a given environment, we identified the nearest asymptomatic trillium of similar size and estimated its predicted seed count (rounded to the nearest whole number) from the relationship between leaf length and seed number using the

predict.glm function; logistical and time constraints prevented us from also sampling seeds from these asymptomatic individuals and determining this relationship directly. Then, we used a negative binomial generalized linear mixed model with seed count as a response, infection status as a fixed effect, and pair number as a random effect.

Within-population infection dynamics

To determine the outcome of phytoplasma transmission at varying host densities within a population, we conducted surveys of trillium density and infection frequency in the *T. grandiflorum* population of KSR (Figure S2) in mid-late May 2018 and 2023. In both survey years, 1 m^2 plots were chosen haphazardly by throwing a flag into the trillium population (Figure S1); all plots in a given year were at least 5 m apart. We grouped subsampling locations on geographic features within the larger population (e.g., separate hill slopes). In 2018, we sampled 210 plots across 21 subsample regions; we counted the number of flowering *T. grandiflorum* in the plot and their infection status based on petal virescence. In 2023, we sampled 64 additional plots across 8 subsample regions with the aim of including more high-density populations and surveying potential vectors. We counted the number of non-flowering and flowering *T. grandiflorum* individuals that had at least three leaves, noted whether phytophagous Hemiptera nymphs were present on the plants, and noted the infection status of flowering trillium. Across both surveys, we estimated the proportion of trillium infected by dividing the number of symptomatic flowering plants by the total number of flowering trilliums (we used only flowering individuals in the denominator because infection was determined by visual petal symptoms). In addition, using data from our 2023 survey, we calculated the proportion of trillium with phytophagous Hemipterans present by dividing the number of trilliums with Hemiptera by the number of trilliums in the plot; we did this for total trilliums and also for only flowering trillium.

To test whether the number of symptomatic trilliums was dependent on the number of flowering trilliums in a patch and sampling year, we used zero-inflated Poisson models with (*GLMMadaptive*; Rizopoulos 2025) and without (*pscl*; Zeileis et al. 2008) a random effect of subsampling location. These zero-inflated models predict both the zeros (infection presence or absence), and the counts (number of symptomatic trillium) separately. We compared the log likelihood of models with and without random effects and used the better fitting model. Then, using data from 2023 only, we used the same models without the year predictor and added the proportion (values between 0-1) of flowering trillium with Hemiptera as an additional predictor. To further explore patterns of trillium density and potential vector occurrence in the 2023 data, we used a binomial generalized linear model with the proportion of trillium with Hemiptera as the response and the total trillium density as the predictor and a weight. Additionally, we used a binomial generalized linear model to test whether the proportion of symptomatic adults in a plot was associated with the proportion of adult trilliums with Hemiptera on them, weighted by total trillium density.

If phytoplasma infection affects seed set then populations may recruit fewer new plants, altering the age class distribution of surrounding plants and challenging long-term population persistence. To determine whether phytoplasma infection affected recruitment and the age class distribution of KSR trillium populations, we first calculated plot level ratios of vegetative to reproductive trillium. We used ratios as responses because they are agnostic to trillium density. Using data from the 1 m^2 plots surveyed in 2023, we calculated the natural log of the ratio of vegetative to flowering three-leaved trillium. Separately, in 2024, we sampled 0.5 m^2 plots centered around the asymptomatic and symptomatic individuals measured for seed production, and recorded the number of one-leaved, three-leaved vegetative, and three-leaved flowering

trillium. We calculated the ratio of one-leaved to three-leaved flowering trillium, and the ratio of vegetative to flowering three-leaved trillium, then, we normalized the ratios by adding one and by applying a natural log transformation. We used the ratios as responses in separate linear models, with the proportion of flowering trillium infected and total number of flowering trillium in the plot as interacting predictors. Next, we used the absolute abundance of one-leaved and three-leaved vegetative trillium as responses in separate Poisson-distributed generalized linear models (each year tested independently), with the same predictors as described above.

Identification of vectors and phytoplasma strain

To identify the phytoplasma present in trillium, we sampled a leaf from a symptomatic flowering plant and extracted DNA using QIAGEN's DNeasy® PowerSoil® Pro Kit. To assess vector identity and abundance, we deployed yellow sticky traps (15.24 cm x 25.4 cm) attached to bamboo poles just above trillium height at 0.5 m above ground (Figure S1). We placed 20 traps across the sampled KSR trillium regions on June 6th 2023, collected them after 6 days, and stored traps at -20□. We counted and collected potential vectors from each trap, and categorized them into morphotypes. We chose 110 insects across potential vector morphotypes and extracted their DNA using QIAGEN's DNeasy® Blood & Tissue Kit, following the protocol for insect specimens. We detected and amplified the 16S rRNA region of phytoplasma in insect and plant samples with a nested polymerase chain reaction (PCR) using two universal phytoplasma primer pairs R16mF2/R1 and R16F2n/R2 (primers and PCR conditions as reported in Gundersen & Lee 1996) and visualised the presence of phytoplasma using gel electrophoresis. We amplified the mitochondrial cytochrome oxidase subunit 1 region of insect samples positive for phytoplasma using the lib220-1/LepR primers (Hajibabaei et al. 2006). The reactions used 1 µL template, 1 µL each of forward and reverse primers, 12.5 µL GoTaq® Master mix (Promega) and 9.5 µL

nuclease-free water). Insect cycling conditions were as follows: 94□ for 60s, then 5 cycles of 94□ for 40s, 45□ for 40s, and 72□ for 60s, followed by 35 cycles of 94□ for 40s, 51□ for 40s, 72□ for 60s, and a final extension of 72□ for 5 mins. We cleaned all PCR products using 0.2 ul Exonuclease I (New England Biolabs, 20U/ul) and 0.2ul calf intestinal alkaline phosphatase (New England Biolabs,10U/ul). Then, to identify the phytoplasma present in plants and the insects that vector it, we performed Sanger sequencing on PCR products (at the Centre for Analysis of Genome Function and Evolution, University of Toronto) and identified the most similar sequences using the National Centre for Biotechnology Information's nucleotide basic local alignment search tool using the megablast algorithm (Altschul et al. 1990, Chen et al. 2015).

Metapopulation infection dynamics

To understand the outcomes of vectored phytoplasma transmission beyond a local population scale, we characterized spatial patterns of phytoplasma infection of *T. grandiflorum* at a range-wide scale and at range margins. First, we collected data from user observations on iNaturalist, then we annotated all visually symptomatic *T. grandiflorum* observations with the observation field “Phytoplasma Infection?=Yes”. On October 7th, 2025, we downloaded all research-grade iNaturalist observations of *T. grandiflorum* from the Global Biodiversity Information Facility (iNaturalist contributors, iNaturalist 2025) and merged them with their associated metadata and observation fields from iNaturalist, downloaded on the same day (data included in supplementary material). In total, this dataset included 36,497 observations between 2012-2025 with 637 symptomatic individuals. We removed observations with missing latitudes or longitudes, observations with low or missing positional accuracy (uncertainty >10,000 m), and observations likely to be erroneous with both a latitude above 20°N and a longitude below 65°W,

resulting in 27,803 observations. To reduce user bias in the dataset, we limited the maximum number of observations per user to 15 by randomly subsampling, reducing the dataset to 24,103 observations. Then, we used *CoordinateCleaner* (Zizka et al. 2019) to remove observations at country centroids, known biological institutions, observations with equal latitudes and longitudes, observations with any zeroes as coordinates, and observations with identical coordinates. After cleaning, the dataset had 23,218 total observations and 384 symptomatic observations. Users contributed a mean 1.89 total observations and a median of 1 total observation. The symptomatic observations were observed by 319 users. We reprojected the coordinates of observations using ESRI:102003, an equal area projection that is appropriate for *T. grandiflorum*'s range.

Next, we examined patterns of trillium observations across its range, and used Bayesian spatial models to link trillium observation density, as well as other environmental and anthropogenic factors, to the likelihood that a trillium observation displayed evidence of a phytoplasma infection. First, we assigned observations to hexagonal grid cells drawn at a scale of 50 km between opposite sides to quantify trillium observation density across the range. Then, we tested for significant spatial clustering of trillium observations and symptomatic trillium using Moran's I and the moran.mc function (*spdep*; Pebesma and Bivand 2023). We visualised grids using the *sf* (Pebesma 2018), *mapview* (Appelhans et al. 2015), and *rnaturalearth* (Massicotte and South 2017) packages. Then, for each observation, we used the *geodata* package (Hijmans et al. 2025) to extract 30-seconds spatial resolution of worldclim bioclimatic variables, cropland distribution (Zanaga et al. 2021), and human footprint circa 2009 (Venter et al. 2016). Next, we used deterministic Bayesian Integrated Nested Laplace Approximation (INLA) models to determine factors predicting a trillium observation's infection status (Rue et al. 2009). INLA

models can effectively account for spatial autocorrelation of data and model continuous spatial processes like disease. We used a model selection procedure to exclude predictors that increased model deviance information criterion (DIC) by >2 (*ggregplot*; Albery 2025), but we did not exclude predictors that we had an *a priori* reason to include, such as footprint and observation density. Then, we removed multicollinear variables using vifcor (*usdm*; Naimi et al. 2014), until all predictors had a variance inflation factor below 5. We fit the base model using predictors of cropland, footprint, total trillium number within the observation's 50 km grid cell, mean diurnal range, temperature seasonality, mean temperature of wettest quarter, mean temperature of driest quarter, mean temperature of warmest quarter, precipitation seasonality, and precipitation of wettest quarter. The binary response variable was the presence or absence of phytoplasma symptoms for each observation. Then, we fit the same model incorporating spatial autocorrelation using a stochastic partial differentiation equation (SPDE) random effect (Lindgren et al. 2011); we set priors following Albery et al. (2020). When the 2.5% and 97.5% posterior estimates of predictors did not overlap zero, we considered this strong evidence that the predictor affected infection. We used the Efxplot and ggField functions (*ggregplot*; Albery 2025) to plot the INLA model fixed results and the spatial field, which represents the marginal posterior mean effects of the spatial random effects on infection status.

Results

Trillium grandiflorum growth and reproduction is reduced by infection

Phytoplasma-infected trilliums were smaller and showed stunted reproduction through altered morphology and loss of functional reproductive structures (Figure 1). Symptomatic trilliums were on average 15.4% shorter than asymptomatic trilliums ($X^2 = 8.77$, $p = 0.003$; Figure S3, Table S1), a difference of 4.26 cm. While the length of leaves was not significantly

different (X^2 = 0.491, p = 0.484; Table S1), sepals were on average 28% longer in symptomatic individuals (X^2 = 25.6, p < 0.001; Figure S3, Table S1). Symptomatic individuals produced on average 5.85 ± 1.18 seeds while asymptomatic trillium produced an estimated 18.5 ± 0.79 seeds (X^2 = 34.7, p < 0.001 ; Figure 2A, Table S2). 63% of symptomatic trillium produced no seeds.

High infection frequency, possibly through lower seed production, reduced the relative abundance of one-leaved trillium stage classes compared to flowering trillium ($F_{1,138}$ = 4.54, p = 0.035; Table S3, Figure 2B). We found no significant effect of infection frequency on the ratio of vegetative to flowering three-leaved trillium in 2023 or 2024 (Table S3). Infection frequency had a non-significant negative relationship with the absolute number of one-leaved trillium in 2024 and vegetative three-leaved trillium in 2023, however it did significantly reduce the number of vegetative three-leaved trillium in 2024 ($F_{1,138}$ = 5.28, p = 0.022; Table S4). As expected, flowering trillium significantly increased the abundance of vegetative three-leaved trillium in 2023 ($F_{1,62}$ = 228, p < 0.001) and 2024 ($F_{1,138}$ = 60.3, p < 0.001). The number of one-leaved trillium was only affected by the interaction between infection frequency and number of flowering trillium; flowering trillium counteracted the negative effect of infection frequency ($F_{1,138}$ = 23.6, p < 0.001).

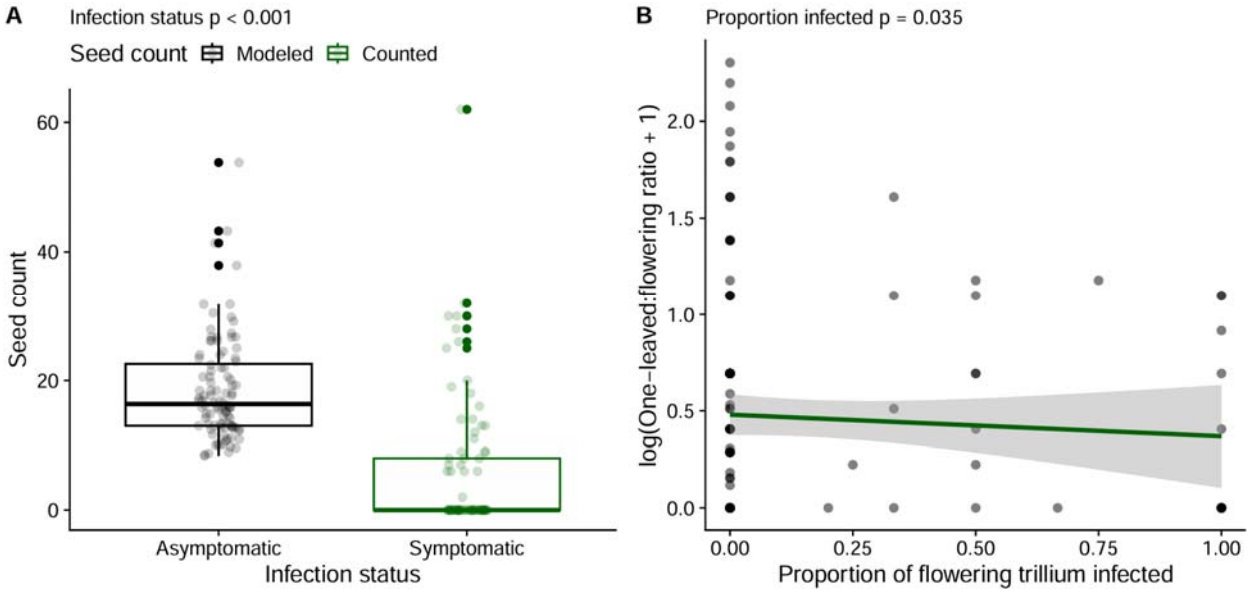

Figure 2. Phytoplasma infection reduced trillium reproduction and the relative abundance of the one-leaved stage class. Symptomatic plants made fewer seeds compared to nearby asymptomatic trillium ($X^2 = 51.0$, $p < 0.001$) (A). The boxplots show the median with the lower and upper hinges corresponding to the 25th and 75th percentiles, and the upper and lower whiskers represent the largest or smallest value, respectively, that is no further than 1.5 times the inter-quartile range from the hinge. Individual data points represent either direct seed counts ("counted") or seed counts predicted based on an empirical relationship between leaf size and seed set ("modeled"); these points are shown at lower opacity superimposed on the boxplots. In 2024, the ratio of one-leaved trillium to flowering three-leaved trillium declined slightly but significantly across plots with higher infection rates, suggesting that local infection rate detectably altered recruitment (B). The scatterplot shows data points and a linear model fit.

Negative density-dependent infection within populations

Phytoplasma infection within populations was more likely at low densities of trillium, indicating negative density-dependent dynamics (Figure 3AB). Our survey plots included a wide

range of densities (2-74 flowering trillium per 1 m^2) and infection prevalence of flowering trillium ranged from 0% to 21% among plots (Figure 3A). The zero-inflation component of the model indicated that the presence of infection was significantly more likely when flowering trillium were at low density (*z*-value = 2.56, $p = 0.010$; Figure 3B, Table S5) and more likely in 2023 compared to 2018 (*z*-value = -2.07, $p = 0.038$). The count component of the model found no significant effect of year (*z*-value = 0.377, $p = 0.706$; Figure 3C, Table S5) or flowering trillium density (*z*-value = 1.81, $p = 0.069$) on the number of infected trilliums in a plot. Thus, both the probability of infection presence and the proportion of symptomatic individuals was higher at lower densities. When we modelled data from only 2023 and included the prevalence of Hemiptera on flowering trillium as a predictor in the model, we found that an increased prevalence of Hemiptera was marginally associated with an increase in the number of symptomatic trillium (*z*-value = 1.86, $p = 0.063$; Table S6). Consistent with our analysis of both years, we found that symptomatic trilliums were more likely to be present in plots with low densities of reproductive stage trillium (*z*-value = 2.22, $p = 0.026$; Table S6). The zero-inflated model characterising infection across both sampling years had a better fit with the inclusion of categorical location as a random effect (log likelihood of -254.8 compared to -272.1), but for models using only 2023 data we excluded random effects of categorical location as this improved fit (log likelihood -82.6 compared to -83.3).

The density of trillium in patches influenced the prevalence of insect vectors on trillium hosts. As total trillium density increased in a plot, the proportion of total trilliums with Hemiptera nymphs decreased (z-value = -10.786, $p < 0.001$, Figure 3D, Table S7). As the proportion of flowering trillium with Hemiptera increased in a plot, the proportion of

symptomatic trillium also increased (z-value = 4.65, $p < 0.001$, Figure 3E, Table S7). Hemiptera were highly prevalent and occurred on 42% to 100% of flowering trillium (Figure 3E).

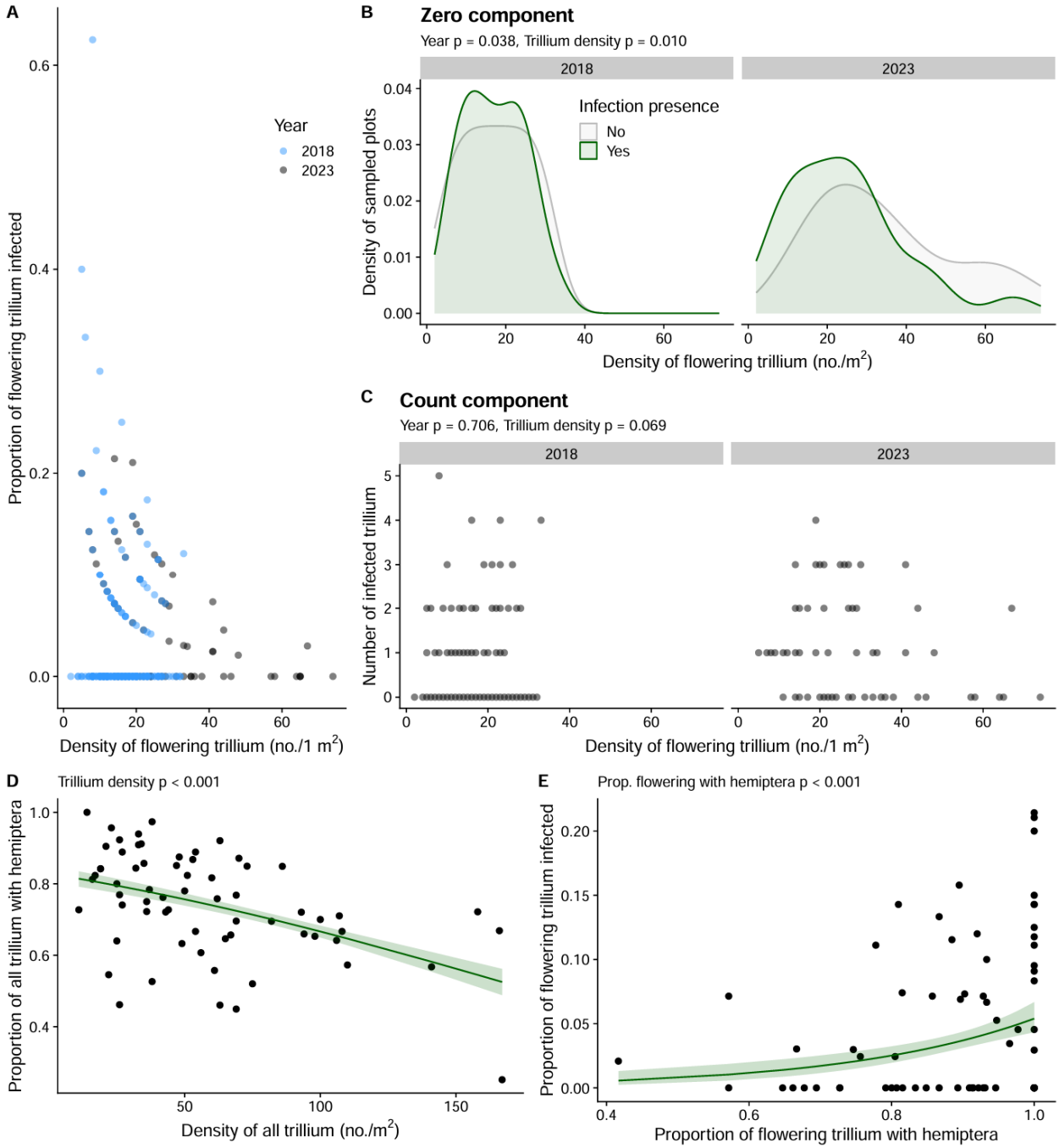

Figure 3. Density-dependent phytoplasma infection patterns within temperate forest populations at Koffler Scientific Reserve (Ontario, Canada). Panel A shows a negative relationship between

the density and infection of flowering trillium, which we tested using a zero-inflated model (BC). Panel B uses a kernel density estimate to show the density of sampled plots along different trillium densities, coloured by whether there were one or more symptomatic trilliums in the plot. At lower trillium densities infection presence in a plot is more likely, while at higher trillium densities, plots are less likely to contain symptomatic trillium (B); significance values are from the binomial component of a zero-inflated model. When infection was present in a plot, the number of infected trilliums was not significantly predicted by trillium density or year (C); significance values are from the count component of a zero-inflated model. In 2023, trillium in less dense patches were more likely to be found with phytophagous Hemiptera nymphs (D), and rates of infection were higher in plots where more plants had phytophagous Hemiptera (E). The scatterplots in D and E show data points and fits from binomial generalised linear models.

Phytoplasma strain was vectored by multiple leafhopper morphotypes

The strain of phytoplasma in *T. grandiflorum* plants at KSR was *Candidatus* Phytoplasma pruni-related, group 16SrIII; the closest identity match had >95% similarity and was to the phytoplasma previously identified in white trillium by Arocha-Rosete et al. (2016). In total, we captured 906 insects in the order Hemiptera from the sticky traps, including 14 morphotypes of leafhoppers (Hemiptera: Cicadellidae). Of the 110 insects tested for phytoplasma presence, we found 4 individuals across 2 leafhopper morphotypes that carried phytoplasma infection at KSR (Figure 1GH; Figure S4; Table S8). The phytoplasma-positive insect specimens had >96.6% sequence similarity to leafhoppers in the *Empoasca* genus. Further details and sequences are provided in the supplement (Table S8; Supplemental file) and on the Sequence Read Archive (BioProject PRJNA1321329).

Phytoplasma is prevalent across Trillium grandiflorum range

Trillium observations and infection were spatially structured and clustered across the landscape (Monte-Carlo simulation of Moran's I $p = 0.001$ for each, Figure 4AB). Symptomatic trillium observations were more clustered than trillium observations at large (Moran's I of 0.376 compared to 0.308). Despite clustering, we found observations of phytoplasma infection at almost all putative range edges of trillium, even when there were relatively few observations in total (Figure 4AB). The northern range edge showed the least evidence of infection (Figure 4B), with the model predicting low likelihood of infection north of 46°N (Figure 4C). The INLA model spatial field, representing the marginal posterior mean effects of the spatial random effects on infection, indicated a high likelihood of infection across the range of *T. grandiflorum*, especially in the central, southern, and western parts of the range (Figure 4C; standard deviation shown in Figure S5). The spatial model indicated that higher mean temperatures of the warmest quarter were negatively correlated with the likelihood of an observation's infection (mean effect -0.451, credible interval of -0.721 to -0.191) and cropland cover was positively associated with an increased likelihood of an observation's infection (mean effect 1.49, credible interval of 0.833 to 2.14) (Figure 4D; Table S9). All other predictors in the spatial model were not associated with likelihood of infection, including the number of trillium observations nearby and human footprint. All predictors had credible intervals non-overlapping with 0 in the base INLA model without spatial structure, except observation density, precipitation seasonality, and mean temperature of the wettest and driest quarters (Figure 4D; Table S10). INLA model fit was substantially improved by incorporating spatial random effects (ΔDIC = 230).

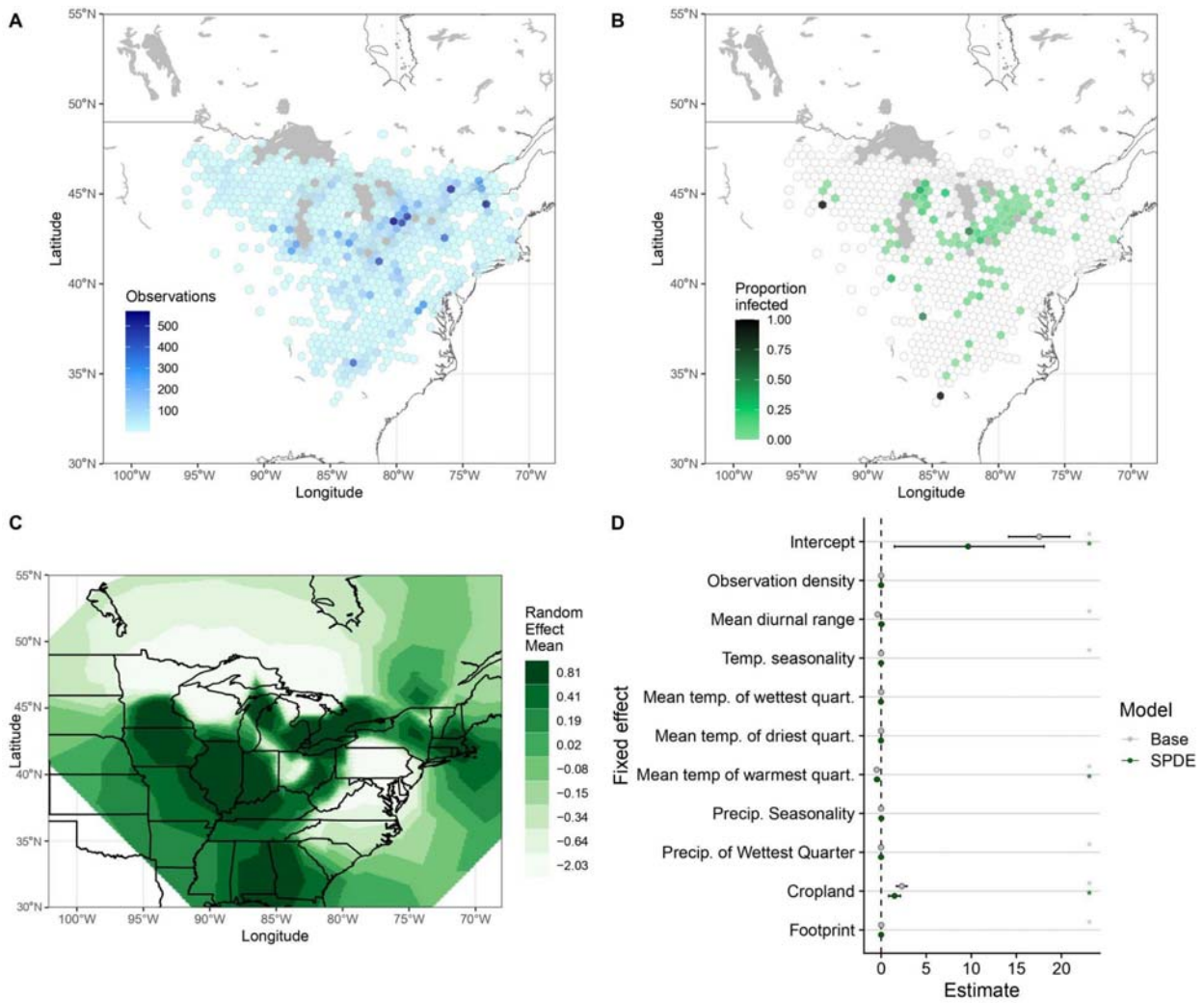

Figure 4. Patterns and predictors of phytoplasma infection across the range of *Trillium grandiflorum*. The dataset had 23,218 observations (A) with 384 observations of phytoplasma-symptomatic plants (B). The 50 km^2 hexagonal grid in (A) and (B) represents areas with at least one observation of *T. grandiflorum*; shading in (B) represents the proportion of observations in that hexagon that show symptoms, and white hexagons had no symptomatic observations. The INLA spatial field (C) represents the effect that spatial position had on infection accounting for all other covariates in the model. Spatial effects on infection were generally positive, particularly in the southern and western parts of the range (C). Cropland cover and mean temperature of the warmest quarter were significantly associated with increased and decreased trillium infection

respectively in the model that accounted for spatial autocorrelation (SPDE) (D). Asterisks in (D) indicate that the effect and its confidence intervals do not overlap zero in that model; the model is indicated by asterisk colour, with light grey representing the base model and dark green representing the spatial model. Abbreviations are as follows: min. = minimum, temp. = temperature, precip. = precipitation, quart. = quarter.

Discussion

We studied the impacts of a sterilizing, vector-transmitted pathogen on white trillium populations and patterns of infection across trillium's range. Within populations, we found that phytoplasma infection presence was more likely in low host density plots, where insect vectors occupied a higher proportion of trillium. The absolute number of symptomatic trilliums was similar across all plots that had infection present, such that low density plots had a greater proportion of symptomatic individuals. Phytoplasma infection was widely distributed across trillium's range and was associated with temperature and proximity to cropland. Below, we discuss the ecological processes at work, and their potential consequences for white trillium and other plant populations.

Patterns and processes of phytoplasma within and across white trillium populations

One possible mechanism driving negative density-dependent patterns within populations is the encounter-dilution effect (Mooring and Hart 1992, Krebs et al. 2014), wherein vectors may satiate or saturate or are otherwise unable to occupy all hosts at high host densities (Gilbert 2002). Indeed, our results support vector limitation because Hemipteran nymphs occupied a lower proportion of trillium at higher host densities (Figure 3D), and nymph presence is likely a good direct and indirect proxy for vector visitation and contact. As suggested by theory and other recent empirical work (Antonovics et al. 1995, 2023, Bruns et al. 2019b), our results provide support for the idea that the encounter-dilution effect, a density-dependent process, affects the outcome of vectored disease in a natural plant population. It is also possible that infected trillium could experience higher mortality or regression to dormancy than non-infected individuals, leading to sparser patches over time where transmission is high, and further compounding the encounter-dilution effect. Higher mortality or regression did not lead to changes in stage class

structure, however, which we discuss more below. If phytoplasmas are transmitted in a negative density-dependent manner, they may be more difficult to eradicate from host populations, because efforts to reduce their abundance by removing infected hosts can lead to the very conditions that promote the fastest phytoplasma population growth, ultimately increasing their resilience (Churcher et al. 2006).

The community science data and the spatial model demonstrated that this vectored pathogen is not constrained to specific regions of the host range, providing evidence that disease can be maintained at both the core and edges (Bruns et al. 2019a) and potentially limit host species ranges. There may be several contributing factors creating this pattern. First, if vectored pathogens are more able to colonize small and low-density host populations compared to other types of pathogens, that may lead to reservoirs of infection that bridge populations. Secondly, while leafhoppers often disperse a few dozen meters a day (Zhou et al. 2003), they can occasionally disperse long distances using wind-mediated migration (Santos et al. 2024), meaning that phytoplasma may be less dispersal-limited compared to aerially or contact transmitted pathogens. Finally, vectored pathogens also benefit from the intelligence of their vector, as many insects are experts at seeking out their host plants in the environment (Webster and Cardé 2017, Jones et al. 2022). At the landscape scale, vectors may find plant hosts based on the frequency of the host relative to other plant species (Antonovics et al. 1995), aligning with processes occurring in frequency-dependent transmission. We did not design our study to explicitly test whether phytoplasma infection at the range scale correlates with trillium density because iNaturalist observation density does not necessarily correlate with trillium population size or density. Regardless, our work suggests that phytoplasma transmission maintains infection

at most range edges and motivates more experimental work to understand range-level drivers of vectored pathogens.

Several environmental factors predicted phytoplasma infection at the range-wide scale. We found that higher mean temperatures of the warmest quarter correlated with reduced chance of infection, which was unexpected given the hypothesized relationship between heat stress and plant infection susceptibility (Hector et al. 2022). High heat could correlate with some other aspect of phytoplasma ecology, perhaps through vector identity, activity levels or phenology, or cool areas may coincide with historical regions of disease introduction. Additionally, we found that cropland cover was associated with increased likelihood of infection in *T. grandiflorum*. Phytoplasmas are a major problem in agricultural crops (Munyaneza and Henne 2013, Rao et al. 2018), and our result suggests that infection may spread from farms and into wild populations, and vice versa, and that the successful management of phytoplasma must consider both environments.

Caveats of spatial data

Combining community science data and hypothesis-driven field work is an especially powerful way to understand disease dynamics and patterns in plants (Meentemeyer et al. 2015). Using community science data allowed us to survey phytoplasma infection in trillium across an otherwise intractable number of plants and locations. The observations showed spatial clustering likely due to the real structure of trillium populations as well as biases like human population density and location accessibility. Human footprint and the number of trillium observations were weakly positively correlated, however neither were significant predictors in the spatial INLA model, suggesting that the increased sampling effort alone did not change the likelihood of an observation's infection status. If symptomatic trilliums were more likely to be documented than

non-symptomatic trillium, this may have increased the likelihood of phytoplasma detection in populations. Additionally, the full range of abiotic factors experienced by trillium were likely not captured or evenly sampled by our community science data (Figure S6), due to human bias in location; when some values of the predictor space are more sparsely sampled, this may make it harder to detect relationships between predictors and response, or between predictors. To help reduce these biases, our model selection procedure removed predictors with significant collinearity, making it less likely that our significant geographic predictors are being driven by other predictors such as human footprint and nearby observation number. Finally, our spatial analysis modelled the chance that an observation was symptomatic, and it provided an estimate of how continuous space affected that probability. While we present the proportion of trillium observations with symptoms over space for visualization purposes (Figure 4B), the proportions are not meant to reflect actual phytoplasma infection frequencies within those populations, nor have we attempted to model infection frequency directly with our model. So, while there are limitations to what we can infer with our spatial data, the disease phenotype remains a strong indicator of phytoplasma presence across the majority of trillium range.

Implications of phytoplasma on plant ecology and evolution

Given the high fitness cost accrued with phytoplasma infection and given that leafhoppers transmit the parasite through a form of herbivory, we predict that plant traits involved in herbivore attraction and defense are under selection (Mauricio and Rausher 1997, Agrawal 2011). However, white trillium does not appear to have many physical defenses against herbivory (Figure 1) and its chemical defense remains unknown. Deer herbivory is known to play a role in structuring trillium populations (Knight 2003, 2007), in contrast, insect herbivory remains largely unstudied (but see Rathcke 1985). It is clear phytoplasma affects fitness

components through direct sterilization and conceivably by pollinator avoidance (due to altered floral morphology). Thus, phytoplasma has the potential to change the selective landscape of plants, and more research is needed to understand if there is any subsequent phytoplasma-mediated selection on plant traits in trillium populations, and how this interacts with other important processes such as growth, pollination, and seed dispersal.

Implications of phytoplasma on wild plant population persistence

Infection may have consequences for trillium population persistence. Because phytoplasma is sterilizing and prevalent across trillium's range, it may reduce white trillium population size in both core and edge populations (Antonovics 2009). Drift, which erodes genetic variation over time, is stronger in small populations (Star and Spencer 2013), meaning that the adaptive capacity of populations may be negatively impacted by prevalent infection. If edge populations are smaller or more isolated than central populations, they may particularly struggle under further reduced population sizes, lower adaptability, and high risk of infection (Bahn et al. 2006). Edge populations can harbour genotypes adapted to a wider range of abiotic conditions (Rehm et al. 2015), and their preservation may be important for the ability of white trillium to expand its range and track shifting climates. Additional populations of conservation concern are the endangered species of trillium that overlap in range with *T. grandiflorum* (Meredith et al. 2022). We have reason to suspect many *Trillium* species are susceptible to phytoplasma because both *T. grandiflorum* and *T. erectum* were identified as hosts by Arocha-Rosete et al. (2016).

Despite theory predicting high rates of local extinction due to a sterilizing pathogen in a long-lived species (Anderson and May 1981, Boots et al. 2002, Gerber et al. 2005, Antonovics 2009), the trillium populations at KSR remain productive after hosting phytoplasma for more

than 20 years, though the amount of change in spatial structure, absolute trillium abundance, and infection prevalence over that time remains unknown. At the patch level, only the relative abundance of the one-leaved stage class was affected by infection, but the effect was not large (Figure 2B). We may not see a larger shift in demographic structure because long-lived populations could experience high lag, or because the KSR populations remain large enough that the reduced seed input is not yet materially affecting recruitment rates. Our plots were smaller than the seed dispersal kernel of trillium (Kalisz et al. 1999, Vellend et al. 2003), so it's likely that plots with high infection received seed subsidies from surrounding areas. The reduced number of three-leaved vegetative trillium in plots with high infection could suggest that reproductive infected trilliums are dying or regressing to dormant stages at the same rate that younger classes are not being recruited, leading to stable stage classes with an overall reduction in trillium abundance. Regression to dormancy can be instigated by other stressors like deer herbivory (Knight 2003). Another alternative explanation is that trilliums continue to reproduce by rhizomes, masking the demographic consequences of plants producing fewer seeds. However, whether infected trillium continue to produce rhizomes and whether rhizomes perpetuate the systemic infection is unknown (Lee et al. 2000, Ustun et al. 2023). Multiple modes of transmission may compound the difficulties small populations may face (Uricchio et al. 2023), and lead to an even higher likelihood of local extinction while providing a veneer of stability. The full demographic consequences of phytoplasma infection may have yet to materialize.

Literature cited

Afkhami, M. E., P. J. McIntyre, and S. Y. Strauss. 2014. Mutualist-mediated effects on species' range limits across large geographic scales. Ecology Letters 17:1265–1273.

Agrawal, A. A. 2011. Current trends in the evolutionary ecology of plant defence. Functional Ecology 25:420–432.

Albery, G. 2025. ggregplot: R package. https://github.com/gfalbery/ggregplot.

Albery, G. F., C. Newman, J. B. Ross, D. W. MacDonald, S. Bansal, and C. Buesching. 2020. Negative density-dependent parasitism in a group-living carnivore. Proceedings of the Royal Society B: Biological Sciences 287:20202655.

Alexander, H. M. 2010. Disease in Natural Plant Populations, Communities, and Ecosystems: Insights into Ecological and Evolutionary Processes. Plant Disease 94:492–503.

Altschul, S. F., W. Gish, W. Miller, E. W. Myers, and D. J. Lipman. 1990. Basic local alignment search tool. Journal of Molecular Biology 215:403–410.

Anderson, R. M., and R. M. May. 1981. The population dynamics of microparasites and their invertebrate hosts. Philosophical Transactions of the Royal Society of London. B, Biological Sciences 291:451–524.

Antonovics, J. 2009. The effect of sterilizing diseases on host abundance and distribution along environmental gradients. Proceedings of the Royal Society B: Biological Sciences 276.

Antonovics, J. 2017. Transmission dynamics: critical questions and challenges. Philosophical Transactions of the Royal Society B: Biological Sciences 372:20160087.

Antonovics, J., C. R. Amoroso, E. Bruns, and M. Hood. 2023. Host density shapes the relative contribution of vector-based and aerial transmission of a pathogenic fungus. Ecology 104:e3970.

Antonovics, J., Y. Iwasa, and M. P. Hassell. 1995. A Generalized Model of Parasitoid, Venereal, and Vector-Based Transmission Processes. The American Naturalist 145:661–675.

Antonovics, J., A. J. Wilson, M. R. Forbes, H. C. Hauffe, E. R. Kallio, H. C. Leggett, B. Longdon, B. Okamura, S. M. Sait, and J. P. Webster. 2017. The evolution of transmission mode. Philosophical Transactions of the Royal Society B: Biological Sciences 372:20160083.

Appelhans, T., F. Detsch, C. Reudenbach, and S. Woellauer. 2015, December 15. mapview: Interactive Viewing of Spatial Data in R.

Arocha-Rosete, Y., N. P. Morales-Lizcano, A. Hasan, K. Yoshioka, W. Moeder, R. Michelutti, E. Satta, A. Bertaccini, and J. Scott. 2016. First report of the identification of a '*Candidatus* Phytoplasma pruni'-related strain in *Trillium* species in Canada. New Disease Reports 34:19–19.

Bahn, V., R. J. O'Connor, and W. B. Krohn. 2006. Effect of dispersal at range edges on the structure of species ranges. Oikos 115:89–96.

Bates, D., M. Mächler, B. Bolker, and S. Walker. 2015. Fitting Linear Mixed-Effects Models Using lme4. Journal of Statistical Software 67:1–48.

Bell, T., R. P. Freckleton, and O. T. Lewis. 2006. Plant pathogens drive density-dependent seedling mortality in a tropical tree. Ecology Letters 9:569–574.

Boots, M., A. Sasaki, and E. J. Travis. 2002. Parasite□Driven Extinction in Spatially Explicit Host□Parasite Systems. The American Naturalist 159:706–713.

Bruns, E. L., J. Antonovics, and M. Hood. 2019a. Is there a disease-free halo at species range limits? The codistribution of anther-smut disease and its host species. Journal of Ecology 107:1–11.

Bruns, E. L., I. Miller, M. E. Hood, V. Carasso, and J. Antonovics. 2019b. The role of infectious disease in the evolution of females: evidence from anther-smut disease on a gynodioecious alpine carnation. Evolution; international journal of organic evolution 73:497–510.

Burdon, J. J., and G. A. Chilvers. 1982. Host Density as a Factor in Plant Disease Ecology. Annual Review of Phytopathology 20:143–166.

Carlsson, U., and T. Elmqvist. 1992. Epidemiology of anther-smut disease (Microbotryum violaceum) and numeric regulation of populations ofSilene dioica. Oecologia 90:509–517.

Case, F. W. 1993. Trillium grandiflorum. Page Flora of North America North of Mexico [Online]. New York and Oxford.

Chen, Y., W. Ye, Y. Zhang, and Y. Xu. 2015. High speed BLASTN: an accelerated MegaBLAST search tool. Nucleic Acids Research 43:7762–7768.

Christensen, N. M., K. B. Axelsen, M. Nicolaisen, and A. Schulz. 2005. Phytoplasmas and their interactions with hosts. Trends in Plant Science 10:526–535.

Churcher, T. S., J. A. N. Filipe, and M. G. Basáñez. 2006. Density dependence and the control of helminth parasites. Journal of Animal Ecology 75.

Fox, J. and Weisberg Sanford. 2019. An R Companion to Applied Regression. Sage Publications.

Frankel, S. J. 2008. Sudden oak death and Phytophthora ramorum in the USA: a management challenge. Australasian Plant Pathology 37:19–25.

Freckleton, R. P., J. A. Gill, D. Noble, and A. R. Watkinson. 2005. Large□scale population dynamics, abundance–occupancy relationships and the scaling from local to regional population size. Journal of Animal Ecology 74:353–364.

Gates, R. R. 1917. A Systematic Study of the North American Genus Trillium, Its Variability, and Its Relation to Paris and Medeola. Annals of the Missouri Botanical Garden 4:43–92.

Gerber, L. R., H. McCallum, K. D. Lafferty, J. L. Sabo, and A. Dobson. 2005. Exposing extinction risk analysis to pathogens: Is disease just another form of density dependence? Ecological Applications 15.

Gilbert, G. S. 2002. EVOLUTIONARY ECOLOGY OF PLANT DISEASES IN NATURAL ECOSYSTEMS. Annual Review of Phytopathology 40:13–43.

Gilbert, G. S., R. B. Foster, and S. P. Hubbell. 1994. Density and distance-to-adult effects of a canker disease of trees in a moist tropical forest. Oecologia 98:100–108.

Gunton, R. M., and W. E. Kunin. 2009. Density-dependence at multiple scales in experimental and natural plant populations. Journal of Ecology 97:567–580.

Hajibabaei, M., M. A. Smith, D. H. Janzen, J. J. Rodriguez, J. B. Whitfield, and P. D. N. Hebert. 2006. A minimalist barcode can identify a specimen whose DNA is degraded. Molecular Ecology Notes 6:959–964.

Hanzawa, F. M., and S. Kalisz. 1993. The Relationship between Age, Size, and Reproduction in Trillium grandiflorum (Liliaceae). American Journal of Botany 80:405–410.

Hargreaves, A. L., and C. G. Eckert. 2019. Local adaptation primes cold-edge populations for range expansion but not warming-induced range shifts. Ecology Letters 22:78–88.

Harrison, S., and A. D. Taylor. 1997. 2 - Empirical Evidence for Metapopulation Dynamics. Pages 27–42 *in* I. Hanski and M. E. Gilpin, editors. Metapopulation Biology. Academic Press, San Diego.

Harrison, T. L., A. K. Simonsen, J. R. Stinchcombe, and M. E. Frederickson. 2018. More partners, more ranges: generalist legumes spread more easily around the globe. Biology Letters 14:20180616.

Hector, T. E., K. L. Hoang, J. Li, and K. C. King. 2022. Symbiosis and host responses to heating. Trends in Ecology & Evolution 37:611–624.

Hegland, S. J. 2014. Floral neighbourhood effects on pollination success in red clover are scale-dependent. Functional Ecology 28:561–568.

Hijmans, R., M. Barbosa, A. Ghosh, and A. Mandel. 2025, May 31. geodata: Download Geographic Data. https://github.com/rspatial/geodata.

Hooper, G. R., F. W. Case, and R. Myers. 1971. Mycoplasma-like bodies associated with a flower greening disorder of a wild flower, Trillium grandiflorum. The Plant Diesase Reporter 55:1108–1110.

iNaturalist contributors, iNaturalist. 2025. iNaturalist Research-grade Observations. iNaturalist.org. Occurrence dataset https://doi.org/10.15468/ab3s5x accessed via GBIF.org on 2025-10-07.

Jones, L. C., M. A. Rafter, and G. H. Walter. 2022. Host interaction mechanisms in herbivorous insects – life cycles, host specialization and speciation. Biological Journal of the Linnean Society 137:1–14.

Kalisz, S., F. M. Hanzawa, S. J. Tonsor, D. A. Thiede, and S. Voigt. 1999. Ant-Mediated Seed Dispersal Alters Pattern of Relatedness in a Population of Trillium Grandiflorum. Ecology 80:2620–2634.

Kim, T. N., N. Underwood, and B. D. Inouye. 2013. Insect herbivores change the outcome of plant competition through both inter- and intraspecific processes. Ecology 94:1753–1763.

Knight, T. M. 2003. Effects of herbivory and its timing across populations of *Trillium grandiflorum* (Liliaceae). American Journal of Botany 90:1207–1214.

Knight, T. M. 2007. Population-level consequences of herbivory timing in Trillium grandiflorum. American Midland Naturalist 157.

Krebs, B. L., T. K. Anderson, T. L. Goldberg, G. L. Hamer, U. D. Kitron, C. M. Newman, M. O. Ruiz, E. D. Walker, and J. D. Brawn. 2014. Host group formation decreases exposure to vector-borne disease: a field experiment in a 'hotspot' of West Nile virus transmission. Proceedings of the Royal Society B: Biological Sciences 281:20141586.

Kuznetsova, A., P. B. Brockhoff, and R. H. B. Christensen. 2017. lmerTest Package: Tests in Linear Mixed Effects Models. Journal of Statistical Software 82:1–26.

Lamoureux, G., and R. Larose. 2002. Flore printanière: guide d'identification Fleurbec. Fleurbec, Saint-Henri-de-Lévis [Québec].

Lee, I.-M., R. E. Davis, and D. E. Gundersen-Rindal. 2000. Phytoplasma: Phytopathogenic Mollicutes1. Annual Review of Microbiology 54:221–255.

Lee-Yaw, J. A., H. M. Kharouba, M. Bontrager, C. Mahony, A. M. Csergő, A. M. E. Noreen, Q. Li, R. Schuster, and A. L. Angert. 2016. A synthesis of transplant experiments and ecological niche models suggests that range limits are often niche limits. Ecology Letters 19:710–722.

Lindgren, F., H. Rue, and J. Lindström. 2011. An Explicit Link between Gaussian Fields and Gaussian Markov Random Fields: The Stochastic Partial Differential Equation Approach. Journal of the Royal Statistical Society Series B: Statistical Methodology 73:423–498.

Liu, J., D. Gopurenko, M. J. Fletcher, A. C. Johnson, and G. M. Gurr. 2017. Phytoplasmas–The "Crouching Tiger" Threat of Australian Plant Pathology. Frontiers in Plant Science 8.

Lively, C. M., S. G. Johnson, L. F. Delph, and K. Clay. 1995. Thinning Reduces the Effect of Rust Infection on Jewelweed (Impatiens Capensis). Ecology 76:1859–1862.

Massicotte, P., and A. South. 2017, March 21. rnaturalearth: World Map Data from Natural Earth.

Mauricio, R., and M. D. Rausher. 1997. Experimental Manipulation Of Putative Selective Agents Provides Evidence For The Role Of Natural Enemies In The Evolution Of Plant Defense. Evolution 51:1435–1444.

Meentemeyer, R. K., M. A. Dorning, J. B. Vogler, D. Schmidt, and M. Garbelotto. 2015. Citizen science helps predict risk of emerging infectious disease. Frontiers in Ecology and the Environment 13:189–194.

Meredith, C., A. Frances, A. Highland, L. Oliver, A. Floden, L. L. Gaddy, W. Knapp, D. Leaman, S. Leopold, T. Littlefield, R. Raguso, E. Schilling, A. Schotz, A. Walker, and K. Wayman. 2022. The Conservation Status of Trillium in North America. Mt. Cuba Center, and New Mexico BioPark Society, Hockessin, DE and Albuquerque, NM.

Mooring, M. S., and B. L. Hart. 1992. Animal Grouping for Protection From Parasites: Selfish Herd and Encounter-Dilution Effects. Behaviour 123:173–193.

Munyaneza, J. E., and D. C. Henne. 2013. Leafhopper and Psyllid Pests of Potato. Pages 65–102 Insect Pests of Potato. Elsevier.

Naimi, B., N. A. S. Hamm, T. A. Groen, A. K. Skidmore, and A. G. Toxopeus. 2014. Where is positional uncertainty a problem for species distribution modelling? Ecography 37:191–203.

Nathan, P., E. P. Economo, B. Guénard, A. K. Simonsen, and M. E. Frederickson. 2023. Generalized mutualisms promote range expansion in both plant and ant partners. Proceedings of the Royal Society B: Biological Sciences 290:20231083.

Ohara, M. 1989. Life History Evolution in the Genus Trillium. Plant Species Biology 4:1–28.

Oldfather, M. F., and D. D. Ackerly. 2019. Microclimate and demography interact to shape stable population dynamics across the range of an alpine plant. New Phytologist 222:193–205.

Parker, I. M., and G. S. Gilbert. 2018. Density-dependent disease, life-history trade-offs, and the effect of leaf pathogens on a suite of co-occurring close relatives. Journal of Ecology 106:1829–1838.

Pautasso, M., G. Aas, V. Queloz, and O. Holdenrieder. 2013. European ash (*Fraxinus excelsior*) dieback – A conservation biology challenge. Biological Conservation 158:37–49.

Pebesma, E. 2018. Simple Features for R: Standardized Support for Spatial Vector Data. The R Journal 10:439.

Pebesma, E., and R. Bivand. 2023. Spatial Data Science. Chapman and Hall/CRC, New York.

Petersen, S. M., C. Keith, K. Austin, S. Howard, L. Su, and W. Qiu. 2019. A Natural Reservoir and Transmission Vector of Grapevine Vein Clearing Virus. Plant Disease 103:571–577.

R Core Team. 2022. R: A language and environment for statistical computing. R Foundation for Statistical Computing. Vienna, Austria.

Rao, G. P., E. Alvarez, and A. Yadav. 2018. Phytoplasma Diseases of Industrial Crops. Pages 91–121 Phytoplasmas: Plant Pathogenic Bacteria - I. Springer Singapore, Singapore.

Rathcke, B. 1985. Slugs as Generalist Herbivores: Tests of Three Hypotheses on Plant Choices. Ecology 66:828–836.

Rehm, E. M., P. Olivas, J. Stroud, and K. J. Feeley. 2015. Losing your edge: climate change and the conservation value of range-edge populations. Ecology and Evolution 5:4315–4326.

Rizopoulos, D. 2025. GLMMadaptive: Generalized Linear Mixed Models using Adaptive Gaussian Quadrature. https://github.com/drizopoulos/GLMMadaptive.

Rooney, T. P., and K. Gross. 2003. A demographic study of deer browsing impacts on Trillium grandiflorum. Plant Ecology 168:267–277.

Rue, H., S. Martino, and N. Chopin. 2009. Approximate Bayesian Inference for Latent Gaussian models by using Integrated Nested Laplace Approximations. Journal of the Royal Statistical Society Series B: Statistical Methodology 71:319–392.

Santos, A. A., J. Jacques, and E. Pérez-López. 2024. Potential impact of climate change on Nearctic leafhopper distribution and richness in North America. npj Sustainable Agriculture 2:12.

Sinha, R. C., and L. N. Chiykowski. 1980. Transmission and morphological features of mycoplasmalike bodies associated with peach X-disease. Canadian Journal of Plant Pathology 2:119–124.

Smith, E. T. 1879. A Michigan Trillium. Botanical Gazette 4:180–181.

Star, B., and H. G. Spencer. 2013. Effects of Genetic Drift and Gene Flow on the Selective Maintenance of Genetic Variation. Genetics 194:235–244.

Uricchio, L. H., E. L. Bruns, M. E. Hood, M. Boots, and J. Antonovics. 2023. Multimodal pathogen transmission as a limiting factor in host distribution. Ecology 104:e3956.

Ustun, N., M. G. Zamharir, and A. M. Al-Sadi. 2023. Chapter 7 - Updates on phytoplasma diseases management. Pages 97–123 *in* A. K. Tiwari, K. Oshima, A. Yadav, S. A. Esmaeilzadeh-Hosseini, Y. Hanboonsong, and S. Lakhanpaul, editors. Characterization, Epidemiology, and Management. Academic Press.

Vellend, M., J. A. Myers, S. Gardescu, and P. L. Marks. 2003. Dispersal of Trillium Seeds by Deer: Implications for Long-Distance Migration of Forest Herbs. Ecology 84:1067–1072.

Venter, O., E. W. Sanderson, A. Magrach, J. R. Allan, J. Beher, K. R. Jones, H. P. Possingham, W. F. Laurance, P. Wood, B. M. Fekete, M. A. Levy, and J. E. M. Watson. 2016. Sixteen years of change in the global terrestrial human footprint and implications for biodiversity conservation. Nature Communications 7:12558.

Wang, R., B. Bai, D. Li, J. Wang, W. Huang, Y. Wu, and L. Zhao. 2024. Phytoplasma: A plant pathogen that cannot be ignored in agricultural production—Research progress and outlook. Molecular Plant Pathology 25:e13437.

Webster, B., and R. T. Cardé. 2017. Use of habitat odour by host-seeking insects. Biological Reviews 92:1241–1249.

Webster, C. G., B. A. Coutts, R. a. C. Jones, M. G. K. Jones, and S. J. Wylie. 2007. Virus impact at the interface of an ancient ecosystem and a recent agroecosystem: studies on three legume-infecting potyviruses in the southwest Australian floristic region. Plant Pathology 56:729–742.

Wickham, H., M. Averick, J. Bryan, W. Chang, L. McGowan, R. François, G. Grolemund, A. Hayes, L. Henry, J. Hester, M. Kuhn, T. Pedersen, E. Miller, S. Bache, K. Müller, J. Ooms, D. Robinson, D. Seidel, V. Spinu, K. Takahashi, D. Vaughan, C. Wilke, K. Woo, and H. Yutani. 2019. Welcome to the Tidyverse. Journal of Open Source Software 4:1686.

Wright, A.A., M. Shires, C. Molnar, G. Bishop, A. Johnson, C. Frias and S.J. Harper. 2022. Titer and Distribution of '*Candidatus* Phytoplasma pruni' in *Prunus avium*. Phytopathology 112(7):1406-1412.

Zanaga, D., R. Van De Kerchove, W. De Keersmaecker, N. Souverijns, C. Brockmann, R. Quast, J. Wevers, A. Grosu, A. Paccini, S. Vergnaud, O. Cartus, M. Santoro, S. Fritz, I. Georgieva, M. Lesiv, S. Carter, M. Herold, L. Linlin, N. Tsendbazar, F. Raimoino, and O. Arino. 2021. ESA WorldCover 10 m 2020 v100. Meteosat Second Generation Evapotranspiration (MET).

Zeileis, A., C. Kleiber, and S. Jackman. 2008. Regression models for count data in R. Journal of Statistical Software 27.

Zhou, L., C. W. Hoy, S. A. Miller, and L. R. Nault. 2003. Marking Methods and Field Experiments to Estimate Aster Leafhopper (Macrosteles quadrilineaus) Dispersal Rates. Environmental Entomology 32:1177–1186.

Zizka, A., D. Silvestro, T. Andermann, J. Azevedo, C. Duarte Ritter, D. Edler, H. Farooq, A. Herdean, M. Ariza, R. Scharn, S. Svantesson, N. Wengström, V. Zizka, and A. Antonelli. 2019. CoordinateCleaner: Standardized cleaning of occurrence records from biological collection databases. Methods in Ecology and Evolution 10:744–751.

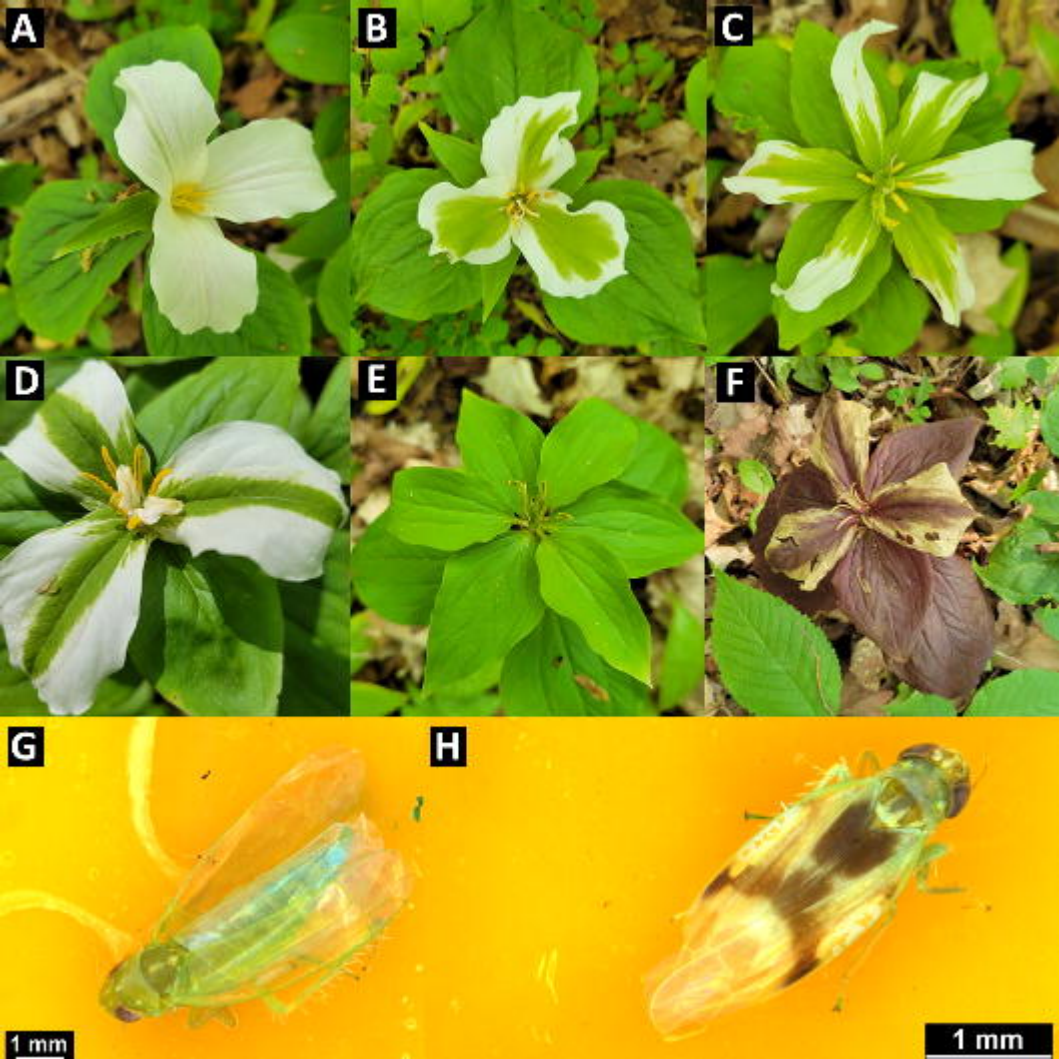
A
B
C
D
E
F
G
H
1 mm
1 mm

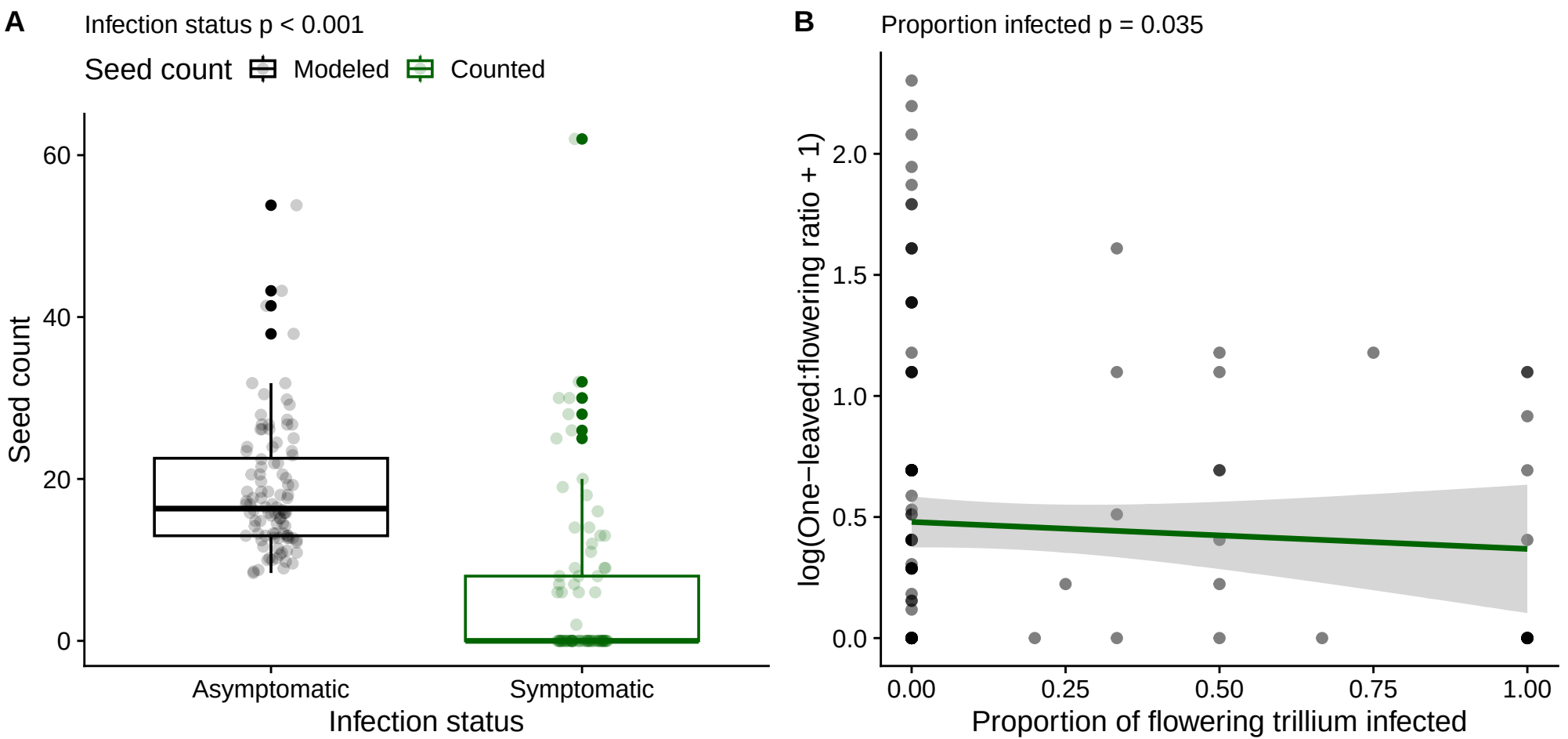
A
Infection status p < 0.001
Seed count
Modeled
Counted
Seed count
60
40
20
0
Asymptomatic
Symptomatic
Infection status
B
Proportion infected p = 0.035
log(One−leaved:flowering ratio + 1)
2.0
1.5
1.0
0.5
0.0
0.00
0.25
0.50
0.75
1.00
Proportion of flowering trillium infected

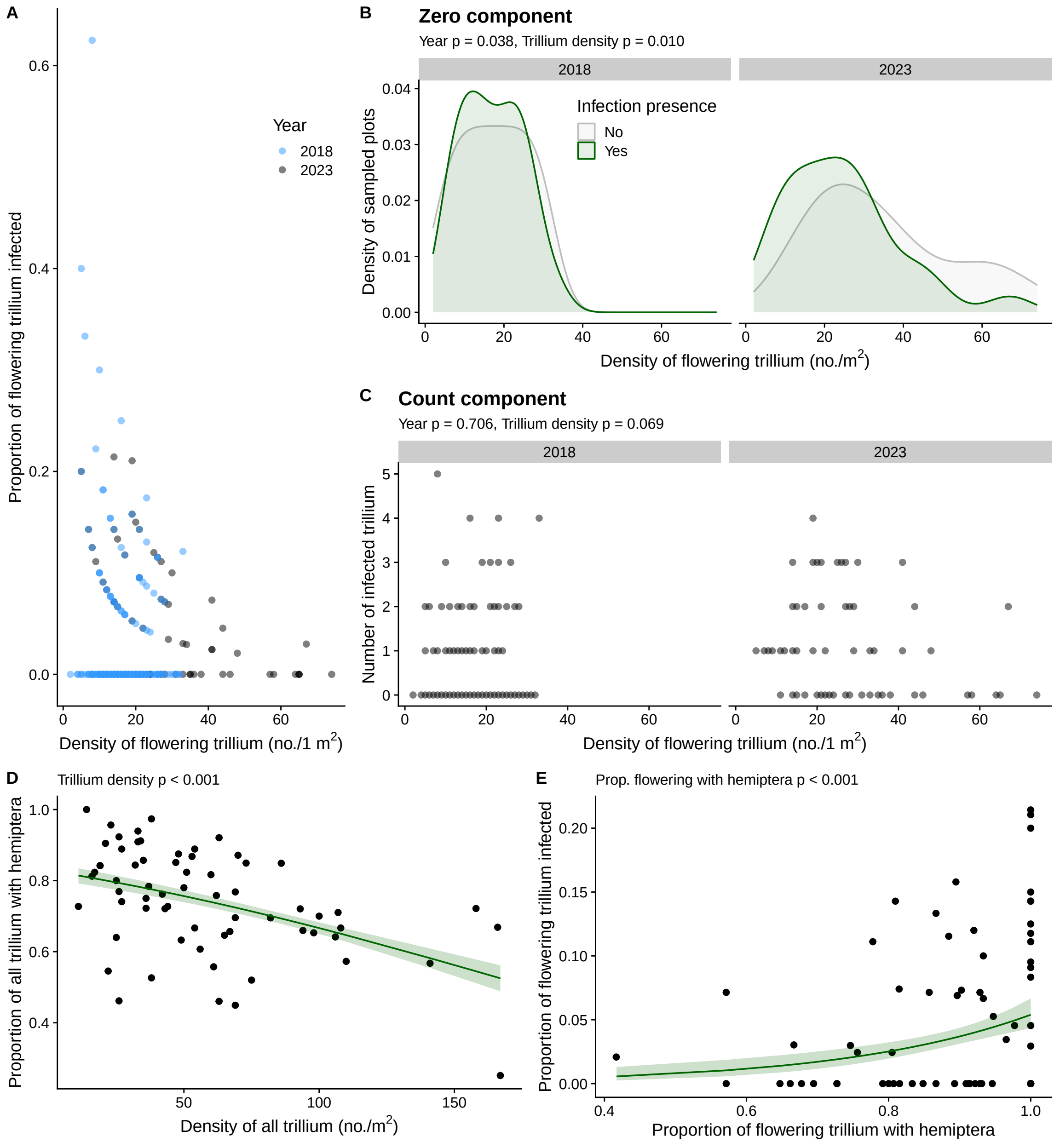
A
Proportion of flowering trillium infected
Density of flowering trillium (no./1 m^2)
Year
2018
2023
B
Zero component
Year p = 0.038, Trillium density p = 0.010
2018
2023
Infection presence
No
Yes
Density of sampled plots
Density of flowering trillium (no./m^2)
C
Count component
Year p = 0.706, Trillium density p = 0.069
2018
2023
Number of infected trillium
Density of flowering trillium (no./1 m^2)
D
Trillium density p < 0.001
Proportion of all trillium with hemiptera
Density of all trillium (no./m^2)
E
Prop. flowering with hemiptera p < 0.001
Proportion of flowering trillium infected
Proportion of flowering trillium with hemiptera

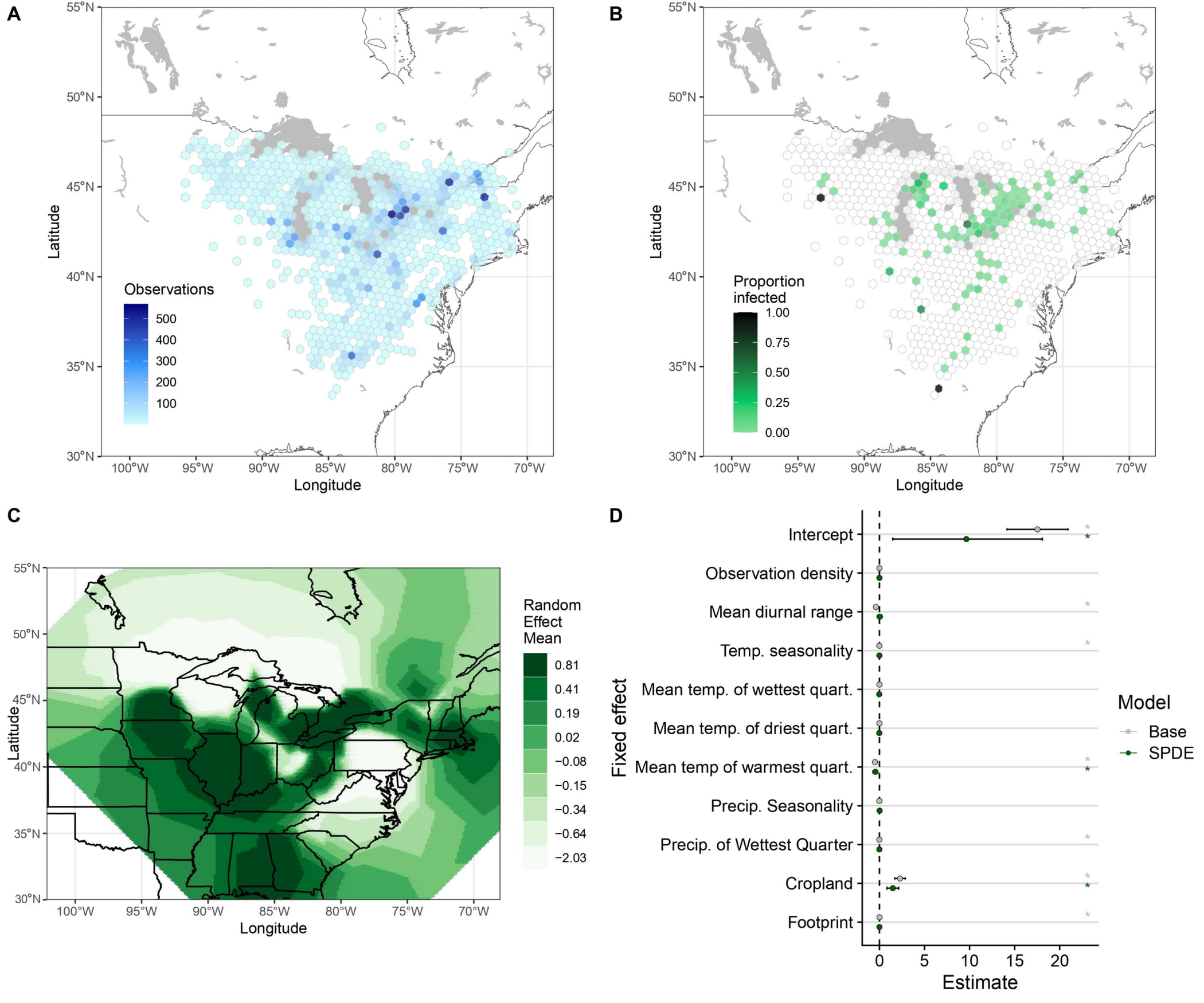
A
Observations
500
400
300
200
100
Latitude
Longitude
55°N
50°N
45°N
40°N
35°N
30°N
100°W
95°W
90°W
85°W
80°W
75°W
70°W
B
Proportion infected
1.00
0.75
0.50
0.25
0.00
C
Random Effect Mean
0.81
0.41
0.19
0.02
−0.08
−0.15
−0.34
−0.64
−2.03
D
Intercept
Observation density
Mean diurnal range
Temp. seasonality
Mean temp. of wettest quart.
Mean temp. of driest quart.
Mean temp of warmest quart.
Precip. Seasonality
Precip. of Wettest Quarter
Cropland
Footprint
Fixed effect
Estimate
0
5
10
15
20
Model
Base
SPDE